Green Synthesis of Silver-Doped Titanium Dioxide Nanostructures for Acetaminophen Degradation Under Solar Radiation[a]

Síntesis verde de nanoestructuras de dióxido de titanio dopadas con plata para la degradación de acetaminofén bajo radiación solar

María Coronell
Universidad de Cartagena, Cartagena, Colombia
ORCID: https://orcid.org/0000-0003-2760-5088

Gina Toscano-Lucas
Universidad de Cartagena, Cartagena, Colombia
ORCID: https://orcid.org/0000-0001-9332-6824

Ricardo Solano
Universidad de Cartagena, Cartagena, Colombia
ORCID: https://orcid.org/0000-0002-4528-2983

Adriana Herrera
Universidad de Cartagena, Cartagena, Colombia
ORCID: https://orcid.org/0000-0002-4355-3401

[a] Research paper - Article of scientific and technological investigation

* Corresponding author. E-mail: aherrerab2@unicartagena.edu.co

Abstract

Objective: In this paper, the photocatalytic degradation of acetaminophen was evaluated using silver-doped titanium dioxide nanoparticles in a cylindrical-parabolic composed photoreactor. *Materials and methods:* Titanium dioxide was synthesized via green synthesis using Cymbopogon citratus leaf extract and doped by silver photodeposition. *Results and discussion:* Morphological information shows that large agglomerates of approximately 49 nm can be attributed to the strong interaction between nanoparticles and their polycrystalline nature. The photodeposition of metallic silver reduces the surface effects, allowing a decrease in the electrostatic interaction and diameter size of the titanium dioxide, as well as the optical properties due to surface poising during the reduction of silver ions to metallic silver. The photocatalytic activity was performed to degrade acetaminophen as the drug model under visible-light radiation. The results are promising, with superior photodegradation of acetaminophen of approximately 37% and 11% for unmodified titanium dioxide and silver-doped titanium dioxide (0.75 at%) nanostructures compared to the commercial photocatalyst, respectively. *Conclusions:* Accordingly, the potential photocatalytic application of silver-doped titanium dioxide nanostructures is highlighted and represents a promising alternative for the photodegradation of organic compounds from wastewater eluents.

Keywords: Sustainable chemistry; surface modification; doping; photocatalysis; pharmaceutical.

Resumen

Objetivo: En esta investigación se evaluó la degradación fotocatalítica de acetaminofén usando nanopartículas de dióxido de titanio dopado con plata en un fotoreactor cilindro parabólico compuesto. *Materiales y métodos:* El dióxido de titanio fue sintetizado a través del método de química verde empleado extracto acuoso de hojas de limoncillo (Cymbopogon citratus) y dopado mediante fotodeposición de plata. *Resultados y discusión:* La información morfológica evidencia aglomeraciones alrededor de los 49 nm atribuido a fuertes interacciones electrostáticas de nanopartículas y su naturaleza policristalina. La fotodeposición de plata metálica reduce los efectos en la superficie permitiendo disminuir la interacción electrostática y el diámetro de las nanopartículas de dióxido de titanio, así como también las propiedades ópticas por envenenamiento superficial durante la reducción de los iones de plata a su estado metálico. La actividad fotocatalítica fue estudiada para degradar acetaminofén como fármaco modelo usando radiación de luz-visible. Los resultados son prometedores con una fotodegradación superior de acetaminofén de 37% y 11% para el dióxido de titanio puro y las nanoestructuras de dióxido de titanio dopadas con plata (0.75 at%) comparado con el fotocatalizador comercial, respectivamente. *Conclusiones:* En este sentido, la potencial aplicación fotocatalítica de nanoestructuras de dióxido de titanio dopadas con plata representa una alternativa prometedora para la fotodegradación de componentes orgánicos en aguas residuales.

Palabras Clave: Química sostenible; modificación superficial; dopaje; fotocatálisis; fármacos

Introduction

Recently, many pharmaceutical and personal care products (PPCPs) have been released into the environment, which is a growing global concern. These PPCPs and their metabolites pose a potential danger to human health and the ecosystem, even at very low concentration levels [1], [2]. Among these, acetaminophen is widely used to relieve mild or moderate headaches, back pain, arthritis, and postoperative pain. It has been detected in concentrations on the order of μg/L in water sources worldwide, as it is one of the most common prescription drugs [3].

The physicochemical properties make acetaminophen very difficult to degrade in drinking water and wastewater treatment plants. To solve this environmental problem, technologies for the elimination of acetaminophen in water sources have been explored, such as constructed wetlands and advanced oxidation processes (ozonation, photoFenton, sonolysis, H_2O_2/UV, heterogeneous photocatalytic processes, and their combinations) [4]–[6]. Heterogeneous photocatalysis is based on the absorption of radiant energy by a semiconductor material, leading to redox reactions and promoting the degradation of organic pollutants. The most commonly used photocatalysts are metal oxides, highlighting titanium dioxide (TiO_2) at the nanoscale since it presents high chemical stability, making it suitable for application over a wide pH range and allowing the production of electronic transitions by light absorption in the near-ultraviolet spectrum [7]. TiO_2 nanoparticles can be synthesized through methods based on the green chemistry paradigm, in which biological sources replace the traditional synthetic and corrosive compounds aiming at facile and environmentally friendly procedures. Green synthesis involves the use of plants [8], agricultural waste [9], fruit shells, among others, which contain different phytochemicals acting as capping, reducing, and stabilizing agents [10].

The high probability of recombination is the aspect that most affects the performance of photocatalytic reactions, as well as the separation between the loads photogenerated by the electron/hole pairs (e^-/h^+) [11]. The resulting redox reactions of material activation are due to the migration of electrons from the valence band to the conduction band, generating e^-/h^+ pairs and promoting reactions to produce hydroxyl radicals. When these reactions are not carried out, either by the absence of dissolved oxygen or adsorbed water, these radicals are recombined by releasing energy attributed to the effect of the absence of dissolved oxygen or adsorbed water during the reaction [12], [13]. Despite the remarkable progress in the development of TiO_2 as a photocatalyst, the practical application is challenged by two limitations inherent in the structure. The first is the low quantum performance, which is determined primarily by the recombination of photogenerated e-/h+ pairs and the bandgap of all TiO_2 phases (3.0–3.2 eV) and essentially responds to the ultraviolet spectrum (4–5% of the solar spectrum) [14], [15]. Second, TiO_2 doping with noble metals, including platinum (Pt), palladium (Pd), gold (Au), and silver (Ag), has been the subject of different studies [16],

[17]. Among these, Ag represents an economical option, acting as an electron trap and promoting interfacial load transfer processes in composite systems. This decreases the recombination of photoinduced e^-/h^+ pairs, improving the photocatalytic activity of TiO_2 [18], [19].

In this study, the photocatalytic degradation of acetaminophen was evaluated using Ag-doped TiO_2 nanoparticles in a cylindrical-parabolic composed photoreactor (CPC). The TiO_2 nanoparticles were synthesized via green chemistry using a *Cymbopogon citratus* (*C. citratus*) leaf extract, followed by surface doping with metallic Ag by photodeposition. The physicochemical properties of the Ag-doped TiO_2 nanostructures were determined using different characterization techniques, including the outstanding polycrystalline nature and the reduction in the diameter size due to Ag doping on the surface. Moreover, experiments related to the photodegradation of acetaminophen showed promising results compared to the performance observed for commercial TiO_2 (P-25) nanoparticles. Finally, this research contributes to the development of novel and eco-friendly methods for materials preparation with photocatalytic activity; in addition, this study represents a starting point for scaling up water resource decontamination processes.

Methodology

Materials

Titanium isopropoxide (95%) and hydrochloric acid (HCl, 37%) were purchased from Alfa Aesar. Silver nitrate ($AgNO_3$, 99.99%) was acquired from Merck, acetaminophen (150 mg/5 mL) from American Generics, reagent alcohol (EtOH, 95%) from "Productos Químicos del Caribe," and sodium hydroxide (NaOH, 99%) from Panreac. Commercial TiO_2 (Degussa P-25) nanoparticles were purchased from Evonik®. Fresh *Cymbopogon citratus* (*C. citratus*) leaves were collected from the rural population of Puerto Escondido, Córdoba, Colombia. Distilled water was used in all experiments.

Cymbopogon citratus extract preparation

C. citratus leaves were washed with distilled water three times to remove other organic content and impurities. The leaves were cut into small pieces, dried in an oven at 40 °C for 6 h, and ground to obtain a powder. Afterward, an infusion was prepared by adding 100 g of the powder to 500 mL of distilled water previously heated at 100 °C. The infusion was then cooled to 60 °C and filtered using a vacuum pump. The concentrated *C. citratus* extract was obtained by reducing the infusion volume up to 100 mL at 80 °C. Finally, the extract was cooled down at room temperature and stored at 5 °C [20].

Green synthesis of titanium dioxide nanoparticles

TiO_2 nanoparticles were obtained via green synthesis using the *C. citratus* extract, which acts as a capping agent for the controlled growth of the rutile phase [20]. Here, a 5 mM solution of titanium isopropoxide was prepared in 85 mL of distilled water under stirring at 175 rpm for 12 h. The solution was then added to 15 mL of the *C. citratus* extract and allowed to react under stirring at 175 rpm for 24 h. Then, the TiO_2 nanoparticles were collected through centrifugation at 5,000 rpm for 10 min. The nanoparticles were purified with several washes with distilled water followed by centrifugation. The crystallization to the TiO_2 anatase phase was completed by drying at 100 °C for 1 h and then annealing at 550 °C for 3 h under airflow.

Synthesis of silver-doped titanium dioxide nanostructures

The Ag-doped TiO_2 nanostructures were obtained through the photodeposition of reduced Ag metal ions on the TiO_2 surface [21]. Three grams of TiO_2 was initially added to 100 mL of deionized water, and the pH was adjusted to 3 using a 0.1 M HCl solution. A concentration of $AgNO_3$ (0.5 at% and 0.75 at%) was then added into the TiO_2 suspension, in which the atomic percentage was previously calculated using *Equation 1*. The suspension was UV-irradiated using a UV-light lamp (30 W G4W T5 Sylvania) under constant stirring for 3 h, aiming to reduce the Ag^+ ions from $AgNO_3$ to metallic Ag. Afterward, the suspension was dried in an oven at 100 °C for 12 h. Finally, TiO_2 doped with 0.5 at% (TiO_2-A) and 0.75 at% (TiO_2-B) Ag was obtained by grinding the particulate matter and annealing at 400 °C for 6 h under airflow.

$$Ag \ at\% = \frac{nAg}{nTi + nAg} \tag{1}$$

where nAg and nTi are the total molar amounts of Ag and Ti ions, respectively [22].

Characterization

The morphology was studied using scanning electron microscopy (SEM) images, which were collected in a Quanta FEG 650 with a field emission gun and an acceleration voltage of 20 kV. Energy dispersed electron (EDX) was used to analyze the elemental composition using an EDAX APOLO X detector coupled to the SEM microscope. The particle size histograms were acquired using the available ImageJ software. The crystal structure was determined from the X-ray diffraction (XRD) pattern collected in an XPert PANalytical Empyrean Series II – Alpha1 using Cu-Kα radiation at room temperature in the 2Θ range of 8-70° with a scan step size of 0.015°. The acetaminophen concentration was determined in a Labomed Inc. UV-2650 spectrophotometer. The UV–Vis diffuse reflectance (UV–Vis/DRS) technique was used to obtain the bandgap using a UV–Visible Shimadzu 2600 spectrophotometer with a

wavelength range of 190 nm-900 nm and a polytetrafluorethylene Spectralon® as a reference.

Photolysis of acetaminophen

Photolysis was used to determine the self-photodegradation and sensitivity of acetaminophen due to sunlight exposure. Initially, a 40 ppm solution of acetaminophen was prepared in 5 L and introduced into a cylindrical parabolic composed photoreactor (CPC). *Figure 1a-c* shows the CPC, consisting of two continuous coupled SCHOTT Duran® borosilicate tubes with a length, external diameter, and thickness of 42 cm, 32 mm, and 1.4 mm, respectively. The acetaminophen solution was pumped using a ½ centrifugal pump horsepower, with a constant recirculation (turbulent regime flow, Re = ~21517) of 6.45 L/min. An aluminum reflective sheet was used inside the CPC to increase the incident sunlight radiation and to be redirected to the borosilicate tubes, aiming to achieve cumulative radiation of 8,000 J/m^2. The cumulative radiation was measured using a photoradiometer (Delta Ohm HD 2102) with an LP-UVB (300 nm-600 nm) probe, and the degradation percentage was calculated from the data collected in a UV–Vis spectrophotometer at 245 nm (absorption maximum wavelength).

Figure 1. Cylindrical parabolic composed photoreactor (CPC) design: (a) full view, (b) top view, and (c) side view.
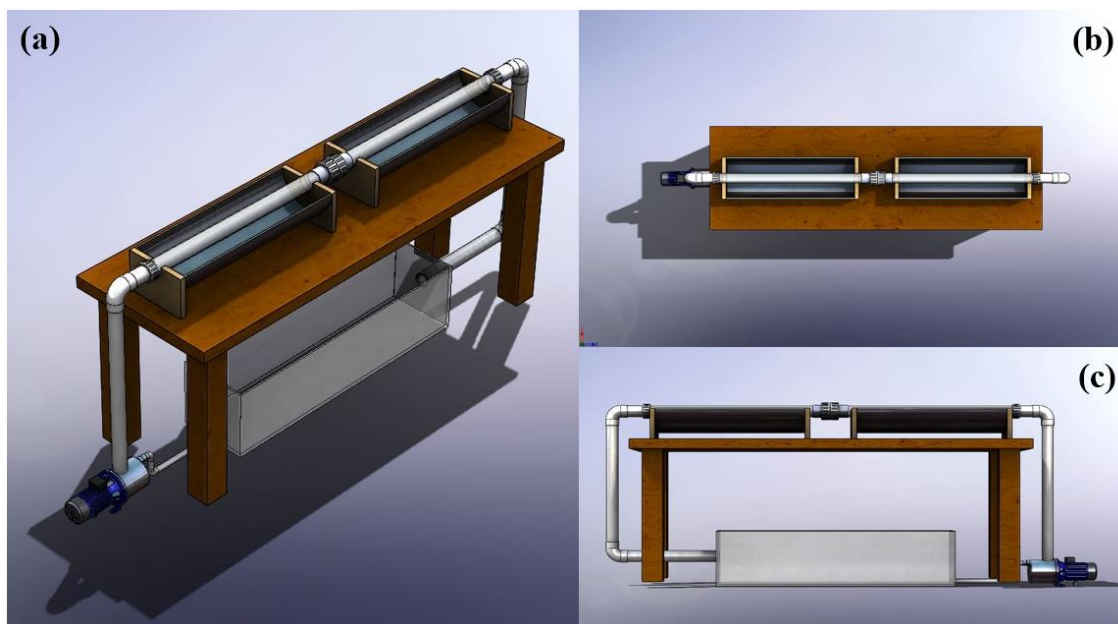
Source: Authors' own creation.

Acetaminophen adsorption on silver-doped titanium dioxide

The potential adsorption of TiO_2-A and TiO_2-B was tested by adding catalyst doses of 0.2 g/L and 0.3 g/L in 2 L of the acetaminophen solution, and commercial TiO_2 was also used to compare the results. The experiments were carried out under constant stirring and covered to avoid exposure to natural light. Aliquots were taken every 15 min for 1 h, each 30 min for 2 h, and one last sample at 3 h. After the samples were centrifuged, the supernatant was stored for UV–Vis analysis (245 nm). The adsorption capacity of Ag-doped TiO_2 was determined to optimize the acetaminophen photodegradation test.

Photodegradation of acetaminophen

The photodegradation of acetaminophen using Ag-doped TiO_2 was evaluated using a CPC (see *Figure 1a-c*). Here, 5 L of the as-prepared acetaminophen solution was introduced into the CPC under the same operational conditions described in the photolysis section. The pH was adjusted to 3 using the HCl solution, reported as the optimum pH_{zpc} for the photodegradation of acetaminophen using TiO_2 nanomaterials [23]. Afterward, TiO_2-A and TiO_2-B were added at catalyst doses of 0.2 g/L and 0.3 g/L, and the CPC was exposed to sunlight irradiation. Commercial TiO_2 was also used to evaluate and compare the photocatalytic performance of Ag-doped TiO_2. Samples were removed every 20 min to calculate the instantaneous radiation (W/m^2) and the cumulative radiation, considering a maximum value of 8,000 J/m^2. The supernatant was collected by centrifugation at 5,000 rpm for 45 min and stored at 4 °C for 24 h. UV–Vis analysis at a wavelength of 245 nm was used to measure the acetaminophen concentration. Finally, *Equation 2* [24] was used to standardize the radiation time (t_{30W}), considering the sunlight UV radiation flux to have a value of 30 W/m^2.

$$t_{30W} = t_{30W,n-1} + \Delta t_n \frac{UV_{G,n}}{30} \frac{V_i}{V_t} \qquad (2)$$

where V_t is the total volume, V_i is the irradiated volume, $UV_{G,n}$ is the average sunlight UV radiation, and $\Delta t_n = (t_n - t_{n-1})$ is the irradiated average time.

Results

Characterization

The crystalline information of the titanium dioxide nanoparticles synthesized via green chemistry and those doped with metallic Ag ions at 0.5 at% (TiO_2-A) and 0.75 at% (TiO_2-B) are shown in *Figure 2*. The TiO_2 nanoparticle pattern shows the characteristic peaks for the tetragonal crystal structure (space Group $I4_1/amd$) of the pure anatase phase. These peaks located at approximately 25°, 38°, 48°, 55°, and 62° correspond to the (101), (004), (200), (105), and (204) planes, respectively, according to the Joint Committee on Powder Diffraction Standards card (JCPDS card no. 00-002-0387) [25]. In the case of Ag-doped TiO_2 nanostructures, three additional peaks (marked with asterisks) can be observed at approximately 28°, 32°, and 46°, which are ascribed to doping with metallic Ag ions and indexed to the (131), (111), and (200) planes with JCPDS card no. 1-1164 [26]. Moreover, these peaks exhibited a significant increase in intensity as the concentration of metallic Ag ions increased on the TiO_2 nanoparticles and showed no effect on the crystal structure of the TiO_2 anatase phase.

Figure 2. X-ray diffraction (XRD) patterns for the identification of the crystal structure of TiO2 nanoparticles and metallic Ag ion doping.
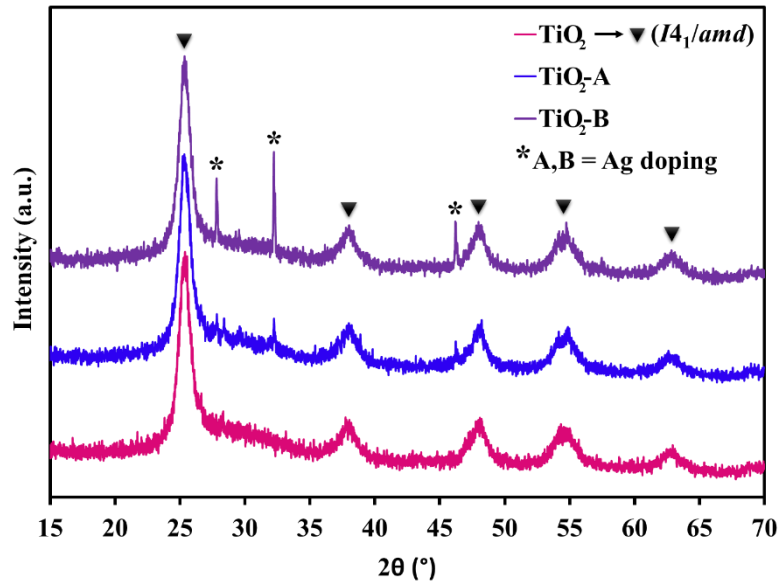
Source: Authors' own creation.

The average crystallite size was estimated using the sharp and intense peaks in the patterns, which corresponded to the different crystalline domains calculated from the Debye-Scherrer *Equation 3* [27].

$$D = \frac{k\lambda}{\beta Cos\theta} \qquad (3)$$

where D is the average crystallite size (nm), k is the Scherrer constant value (0.9), λ is the wavelength in the X-ray (0.1541 nm), β is the full width at half maximum (FWHM, rad), and θ is the Bragg diffraction angle (rad). Accordingly, the average crystallite sizes were 38 nm, 35 nm, and 34 nm with a standard deviation of $\pm$ 19 nm for TiO_2 nanoparticles, TiO_2-A, and TiO_2-B nanostructures, respectively. These values exhibited a low accuracy in the average crystallite size attributed to a possible surface effect, which can lead to a strong agglomeration and a polycrystalline nature. According to previous results, the crystallite size of the anatase phase tends to increase rapidly after 60 min of annealing at high temperature, which promotes an increase in the kinetic energy. This causes the Ostwald ripening effect consisting of the growth and deposition of small crystallites onto large crystallites over time, promoting the formation of polycrystalline TiO_2 nanoparticles with different sizes [28].

The morphology information of the nanomaterials was analyzed from the scanning electron microscopy (SEM) images shown in *Figure 3a-f. Figure 3a,b* shows the formation of small agglomerates of TiO_2 nanoparticles with a semispherical shape and a wide diameter size distribution of approximately 49 $\pm$ 20 nm (see *Figure 4*). Although the *C. citratus* extract played an important role as a capping agent to control growth, the Ostwald ripening effect promoted the formation of large polycrystalline grains from smaller TiO_2 nanoparticles. In the case of the Ag-doped TiO_2 nanoparticles, the presence of smaller agglomerates can be observed. *Figure 3c, d* shows TiO_2 nanoparticles with the photodeposition of 0.5 at% metallic Ag on the surface, obtaining nanostructures with a diameter size of 37 $\pm$ 18 nm (see *Figure 4*). The enhanced dispersion is attributed to the presence of Ag on the surface, leading to the reduction of the surface effect and electrostatic interactions between TiO_2 nanoparticles. Similar results are observed in *Figure 3e, f* regarding the TiO_2 nanoparticles doped with metallic Ag at 0.75 at%. Here, a slight decrease in the diameter size of approximately 31 $\pm$ 17 nm was evidenced from *Figure 4*, corroborating the contribution of metallic Ag in the dispersion of TiO_2 nanoparticles. Despite the small difference in the concentrations used for Ag doping, EDX analysis exhibited a significant increase in the weight content from 14% to 29% when using 0.75 at% instead of 0.5 at%. This is a promising result since the higher the content of metallic Ag on the surface is, the better the photocatalytic activity on the nanostructures by providing more active sites for the photodegradation of acetaminophen.

Figure 3. Scanning electron microscopy (SEM) images of the (a,b) TiO₂ nanoparticles synthesized and those modified with metallic Ag at (c,d) 0.5 at% and (e,f) 0.75 at%.

Element	%W	%at
Ti	20.8	10.0
Ag	14.5	3.1
O	40.6	58.3

Element	%W	%at
Ti	21.9	12.4
Ag	29.0	7.3
O	26.9	45.5
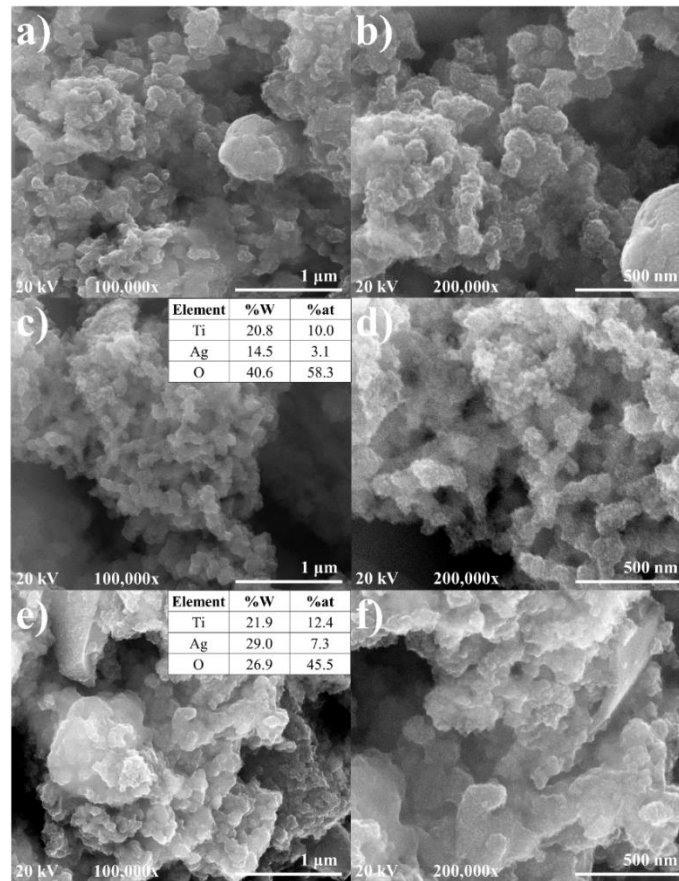
Source: Authors' own creation.

The diffuse reflectance spectra of the Ag-doped TiO₂ nanostructures are shown in *Figure 5*. The visible light absorption showed no improvements after the photodeposition of Ag metal ions on the surface of TiO₂. The absorbance was calculated using *Equation 4* based on the Kubelka-Munk function [29], in which the light absorption decreased due to the inverse relationship with the reflectance. Additionally, the indirect bandgap values were estimated following the Wood and Tauc method described in *Equation 5* [30].

$$F(R) = \frac{(1-R)^2}{2R} = \frac{K}{S} \tag{4}$$

$$F(R)hv \propto \left(hv - E_g\right)^n \tag{5}$$

where $F(R)$ is the absorbance, R is the absolute reflectance, K is the absorption coefficient, S is the scattering coefficient, h is the Planck constant, v is the frequency, and n is the transition value mode. The transition values of 1/2, 2, 3/2, or 3 correspond to the permissible direct, permissible indirect, direct prohibited, and indirect prohibited transition modes,

respectively [31]. The n value is 2 for pure and doped TiO₂ nanoparticles, ascribed to a permissible indirect transition mode [32]. According to Figure 6, the band gap energies were 2.94 eV, 3.08 eV, and 3.10 eV for TiO₂ nanoparticles TiO₂-A and TiO₂-B, respectively.

Figure 4. Particle size distribution histogram of the nanomaterials studied.
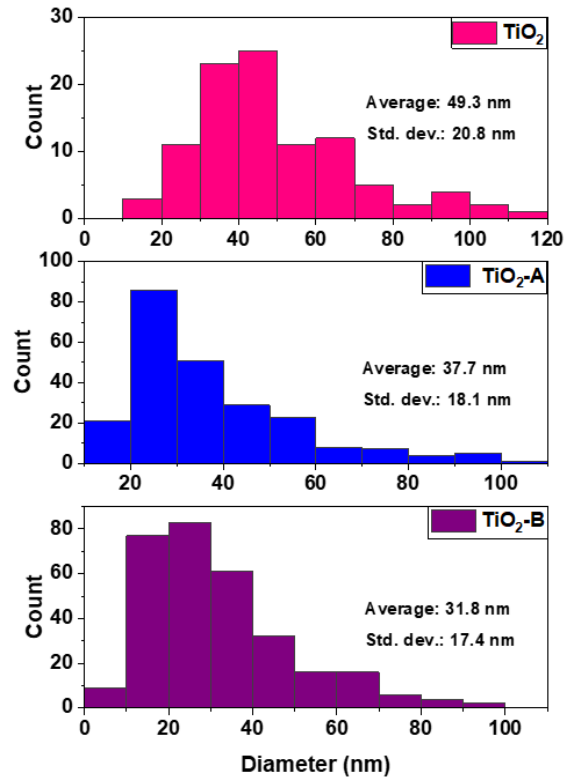
Source: Authors' own creation.

Figure 5. Diffuse reflectance spectrum for TiO2, TiO2-A (0.5 Ag at%), and TiO2-B (0.75 Ag at%).
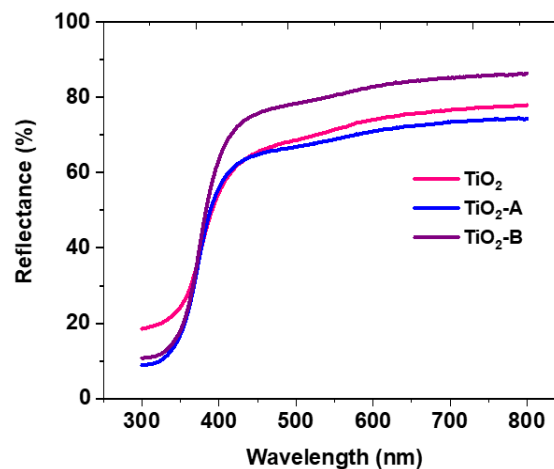
Source: Authors' own creation.

Figure 6. Optical band gap energy estimation (Wood and Tauc method) for TiO2, TiO2-A (0.5 Ag at%), and TiO2-B (0.75 Ag at%) nanoparticles.
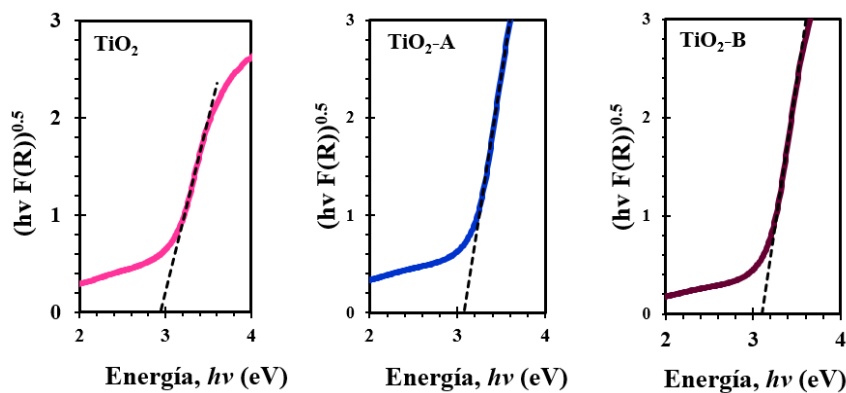
Source: Authors' own creation.

Currently, the literature reports low bandgap energies of TiO_2 nanoparticles doped with Ag ions obtained from different synthesis methods as a result of an electron-hole recombination delay due to the energy states located above the valence band [33]. In this study, the bandgap energy values were significantly higher (see *Table 1*), attributed to the reduction of the electron-hole recombination delay. However, there was no difference between the value for TiO_2 nanoparticles compared to TiO_2-A and TiO_2-B, since the photodeposition method reduced the optical properties through the reduction of Ag^+ ions to metallic Ag [19].

Table 1. Results were reported in recent research related to TiO_2 doping with Ag to improve optical properties.

Synthesis method	Doping amount	Bandgap reduction (eV)	Reference
Green synthesis and photodeposition/reduction	0.5 at% and 0.75 at%	Negligible	This study
Biomediated doping (BMD)	1.0 wt.%	0.70 eV	[34]
Sol-gel method	2 mol% to 8 mol%	0.67 eV	[35]
	1 wt.%, 3 wt.% and 5 wt.%	0.32 eV	[36]
	1.5 wt.%	0.3 eV	[37]
	0.10 mol.%	0.08 eV	[38]
Controlled and energy efficient microwave assisted method	0.12 mol% to 0.5 mol%	0.22 eV	[18]
Sol-gel/solvothermal (SGH)	0.04 Ag/Ti molar ratio	0.25 eV	[39]
Photodeposition method	1.0 wt.%	0.29 eV	[22]

Source: Authors' own creation.

Photocatalytic degradation

The direct photolysis process was performed to determine the sensitivity degree of a 40 mg/L acetaminophen solution exposed to solar irradiation in the absence of the catalyst until a

minimum equivalent radiation of 8,000 J/m^2 was reached. *Equation 6* was used to calculate the degradation percentage in the photolysis, adsorption, and heterogeneous photocatalysis processes [40].

$$Degradation\ (\%) = \frac{C_o - C_t}{C_o} \times 100 \tag{6}$$

where C_o is the initial concentration (mg/L) and C_t is the concentration as a function of time/cumulative radiation. In the results, the photolysis process achieved a degradation rate of 14.5%, showing that the pollutant is slightly susceptible to self-degrade due to exposure to solar radiation. This is an advantage since it represents a savings in terms of photocatalyst material and increases the overall rate during the photocatalytic process. This self-degradation percentage was similar to that reported in other research, which found a reduction of 12% of acetaminophen after irradiation with a mercury lamp (500 W) for 60 min with an initial concentration of 50 mg/L [41].

On the other hand, *Table 2* shows the results obtained from the adsorption experiments avoiding exposure to natural light. Adsorption of acetaminophen with the commercial photocatalyst P-25 was found to be negligible, whereas TiO$_2$ nanoparticles synthesized using the *C. citratus* extract and TiO$_2$-B (0.75 Ag at%) nanostructures showed higher removal percentages due to improvements in their surface area properties. A total surface area of 64.4 m^2/g for TiO$_2$ nanoparticles synthesized via green chemistry using *C. citratus* extract has been previously reported [32], which is 41% higher than that reported for commercial P-25 (45.7 m^2/g) [42]. Moreover, an increased photocatalyst dose decreases the adsorption removal percentage attributed to the surface interaction between the nanoparticles (aggregation), leading to a reduction in the number of available adsorption sites [43], [44].

Table 2. Molecular adsorption percentage of acetaminophen avoiding exposure to natural light and at pH 3 and 40 mg/L after 180 min (equilibrium time).

Material	Catalyst dosage	
	0.2 g/L	0.3 g/L
Commercial P-25	1.7%	1.4%
Green TiO$_2$ nanoparticles	12.7%	7.4%
TiO$_2$-B (0.75 Ag at%)	14.3%	6.7%

Source: Authors' own creation.

The photodegradation tests were performed on consecutive days and at the same time to reduce the variation due to the environmental conditions. *Figure 7a,b* shows the experimental results of acetaminophen photodegradation using photocatalyst doses of 0.2 g/L and 0.3 g/L of commercial P-25, TiO$_2$ nanoparticles, and TiO$_2$-B nanostructures. Additionally, the behavior of the relative C_t/C_0 concentration was evaluated regarding the standardized

radiation time (t_{30w}). At both photocatalyst doses, commercial P-25 presented the lowest degradation efficiency attributed to the adsorption capacity of acetaminophen, whereas TiO_2-B (0.75 Ag at%) showed an intermediate performance due to the photodeposition of metallic Ag ions. In this case, the reduction of Ag^+ ions to metallic Ag promotes surface poisoning of the photocatalyst, leading to a reduction in the photocatalytic activity compared to TiO_2 nanoparticles synthesized via green chemistry. Moreover, the reaction rate decreases considering the high concentration of the photocatalyst (0.3 g/L), which was attributed to a shielding effect from the reduced light irradiation in the innermost part of the reactor [45], [46].

Figure 7. Remaining acetaminophen as a function of the standardized radiation time (t_{30w}) using (a) 0.2 g/L and (b) 0.3 g/L photocatalyst doses.
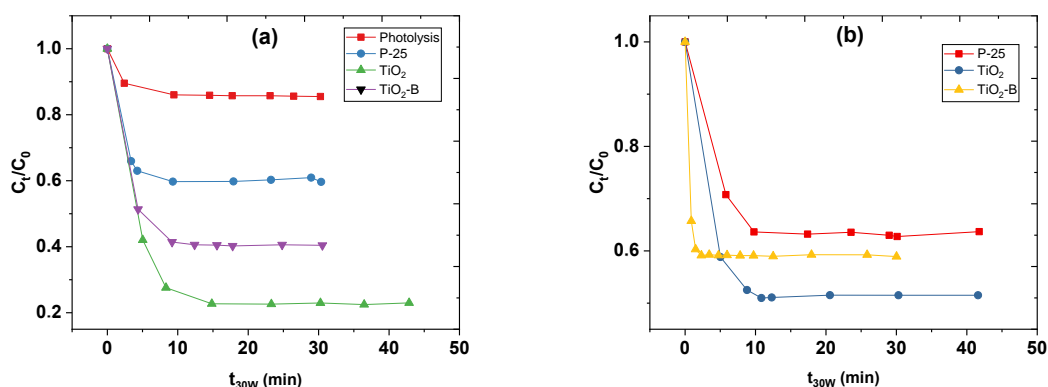
Source: Authors' own creation.

Figure 8. Proposed mechanism by adapting the reported pathways of the photocatalytic degradation of acetaminophen.
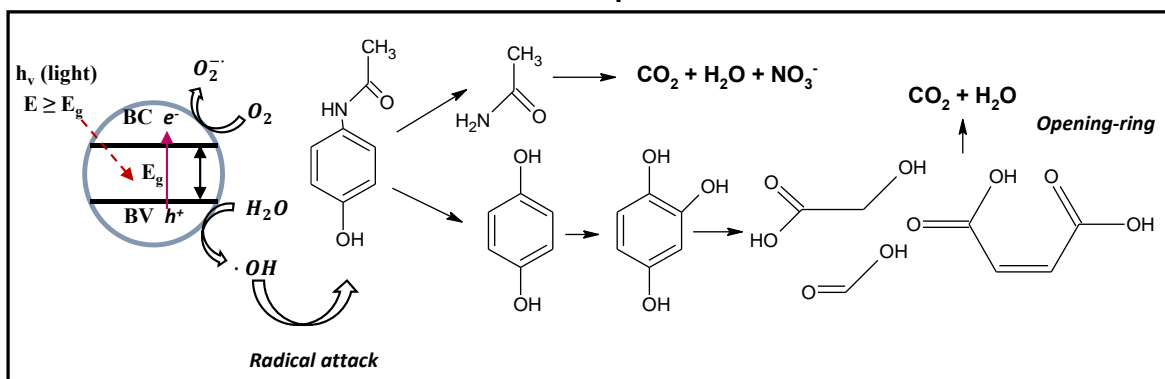
Source: Authors' own creation.

The mechanism for the photodegradation of acetaminophen is displayed in *Figure 8*, which was based on information previously reported in the literature [47, 48]. The mechanism initially consisted of the electron/hollow pair (e^-/h^+) generation from the activation of the

photocatalyst using simulated or natural UV–Vis radiation, as detailed in *Equations 7-12*. Then, the hydroxyl radicals attack the ortho- or para-positions of the aromatic ring in the acetaminophen structure to produce N-Methyl formamide (C_2H_5NO), hydroquinone, and 1,4-benzoquinone. Finally, the opening ring/ring cleavage and the oxidation of species, such as maleic acid ($C_4H_4O_4$), formic acid (CH_2O_2), and glycolic acid ($C_2H_4O_3$), are generated until their mineralization (CO_2 and H_2O).

$$TiO_2 + hv \rightarrow h^+ + e^- \tag{7}$$

$$h^+ + OH^-(surface) \rightarrow OH \cdot \tag{8}$$

$$h^+ + OH^-(adsorbed) \rightarrow OH \cdot + H^+ \tag{9}$$

$$e^- + O_2\ (adsorbed) \rightarrow O_2^{-\cdot} \tag{10}$$

$$O_2^{-\cdot} + H^+ \rightarrow HO_2^{\cdot} \tag{11}$$

$$HO_2^{\cdot} + HO_2^- \rightarrow OH \cdot + OH^- + O_2 \tag{12}$$
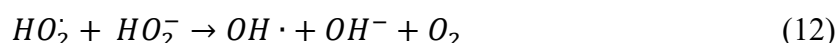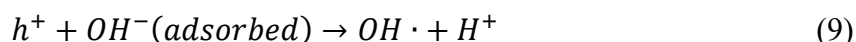
Conclusions

This study reports the green synthesis of titanium dioxide (TiO_2) nanoparticles using a *Cymbopogon citratus* (*C. citratus*) extract as a capping agent and surface modification with metallic Ag via the photodeposition method. Although *C. citratus* acted as a capping agent to control the growth and particle size, the TiO_2 nanoparticles exhibited polycrystallinity attributed to a strong surface effect, leading to the formation of agglomerates with large diameter sizes. The large agglomerates reduce the available active sites for the adsorption of naphthalene since its removal is expected from the photocatalytic degradation instead. On the other hand, the reduction from Ag ions to metallic Ag on the surface of the TiO_2 nanoparticles promoted a direct effect on the optical properties, showing no differences compared to the unmodified TiO_2 nanoparticles. Although this effect caused surface poisoning on the photocatalyst, decreasing the photodegradation of acetaminophen, the results showed a better performance compared to commercial P-25. Therefore, the green synthesis of TiO_2 nanoparticles and photodeposition of metallic Ag on the surface provides an enhanced photocatalytic activity toward the degradation of organic pollutants, in which further research work can involve optimization aiming at better optical properties.

Acknowledgment

References

[1] M. Negarestani, M. Motamedi, A. Kashtiaray, A. Khadir, and M. Sillanpää, "Simultaneous removal of acetaminophen and ibuprofen from underground water by an electrocoagulation unit: Operational parameters and kinetics," Groundw. Sustain. Dev., vol. 11, p. 100474, 2020, doi: https://doi.org/10.1016/j.gsd.2020.100474

[2] J. Diaz-angulo, J. Porras, M. Mueses, R. A. Torres-palma, and A. Hernandez-ramirez, "Coupling of heterogeneous photocatalysis and photosensitized oxidation for diclofenac degradation: role of the oxidant species," J. Photochem. Photobiol. A Chem., vol. 383, p. 112015, 2019, doi: https://doi.org/10.1016/j.jphotochem.2019.112015

[3] Y. Ling, G. Liao, P. Xu, and L. Li, "Fast mineralization of acetaminophen by highly dispersed Ag-g-C3N4 hybrid assisted photocatalytic ozonation," Sep. Purif. Technol., vol. 216, pp. 1–8, 2019, doi: https://doi.org/10.1016/j.seppur.2019.01.057

[4] X. Wang, M. Brigante, W. Dong, Z. Wu, and G. Mailhot, "Degradation of Acetaminophen via UVA-induced advanced oxidation processes (AOPs). Involvement of different radical species: HO[rad], SO4[rad]− and HO2[rad]/O2[rad]−," Chemosphere, vol. 258, p. 127268, 2020, doi: https://doi.org/10.1016/j.chemosphere.2020.127268

[5] R. Mu, Y. Ao, T. Wu, C. Wang, and P. Wang, "Synthesis of novel ternary heterogeneous anatase-TiO2 (B) biphase nanowires/Bi4O5I2 composite photocatalysts for the highly efficient degradation of acetaminophen under visible light irradiation," J. Hazard. Mater., vol. 382, p. 121083, 2020, doi: https://doi.org/10.1016/j.jhazmat.2019.121083

[6] R. Katal, M. H. Davood Abadi Farahani, and H. Jiangyong, "Degradation of acetaminophen in a photocatalytic (batch and continuous system) and photoelectrocatalytic process by application of faceted-TiO2," Sep. Purif. Technol., vol. 230, p. 115859, 2020, doi: https://doi.org/10.1016/j.seppur.2019.115859

[7] J. Shi et al., "Modified TiO2 particles for heterogeneous photocatalysis under solar irradiation," Mater. Lett., vol. 279, p. 128472, 2020, doi: https://doi.org/10.1016/j.matlet.2020.128472

[8] E. K. Kambale et al., "Green synthesis of antimicrobial silver nanoparticles using aqueous leaf extracts from three Congolese plant species (Brillantaisia patula, Crossopteryx febrifuga and Senna siamea)," Heliyon, vol. 6, no. 8, 2020, doi: https://doi.org/10.1016/j.heliyon.2020.e04493

[9] N. Sapawe, N. Surayah Osman, M. Zulkhairi Zakaria, S. Amirul Shahab Syed Mohamad Fikry, and M. Amir Mat Aris, "Synthesis of green silica from agricultural waste by sol-gel method," Mater. Today Proc., vol. 5, no. 10, pp. 21861–21866, 2018, doi: https://doi.org/10.1016/j.matpr.2018.07.043

[10] D. He et al., "One-step green fabrication of hierarchically porous hollow carbon nanospheres (HCNSs) from raw biomass: Formation mechanisms and supercapacitor applications," J. Colloid Interface Sci., vol. 581, pp. 238–250, 2021, doi: https://doi.org/10.1016/j.jcis.2020.07.118

[11] R. M. Castellanos, J. Paulo Bassin, M. Dezotti, R. A. R. Boaventura, and V. J. P. Vilar, "Tube-in-tube membrane reactor for heterogeneous TiO2 photocatalysis with radial addition of H2O2," Chem. Eng. J., vol. 395, p. 124998, 2020, doi: https://doi.org/10.1016/j.cej.2020.124998

[12] A. Cabrera-reina, A. B. Martínez-piernas, Y. Bertakis, N. P. Xekoukoulotakis, A. Agüera, and J. Sánchez, "TiO2 photocatalysis under natural solar radiation for the degradation of the carbapenem antibiotics imipenem and meropenem in aqueous solutions at pilot plant scale," Water Res., vol. 166, p. 115037, 2019, doi: https://doi.org/10.1016/j.watres.2019.115037

[13]   N. J. Ismail et al., "Hydrothermal synthesis of TiO2 nanoflower deposited on bauxite hollow fibre membrane for boosting photocatalysis of bisphenol A," J. Water Process Eng., vol. 37, pp. 1–8, 2020, doi: https://doi.org/10.1016/j.jwpe.2020.101504

[14]   F. X. Nobre et al., "Heterogeneous photocatalysis of Tordon 2,4-D herbicide using the phase mixture of TiO2," J. Environ. Chem. Eng., vol. 7, no. 6, p. 103501, 2019, doi: https://doi.org/10.1016/j.jece.2019.103501

[15]   R. Satish Kumar, K. S. Min, S. H. Lee, N. Mergu, and Y. A. Son, "Synthesis of novel panchromatic porphyrin-squaraine dye and application towards TiO2 combined photocatalysis," J. Photochem. Photobiol. A Chem., vol. 397, p. 112595, 2020, doi: https://doi.org/10.1016/j.jphotochem.2020.112595

[16]   M. R. Al-Mamun, S. Kader, M. S. Islam, and M. Z. H. Khan, "Photocatalytic activity improvement and application of UV-TiO2 photocatalysis in textile wastewater treatment: A review," J. Environ. Chem. Eng., vol. 7, no. 5, pp. 1–17, 2019, doi: https://doi.org/10.1016/j.jece.2019.103248

[17]   R. Qian et al., "Charge carrier trapping, recombination and transfer during TiO2 photocatalysis: An overview," Catal. Today, vol. 335, pp. 78–90, 2019, doi: https://doi.org/10.1016/j.cattod.2018.10.053

[18]   M. B. Suwarnkar, R. S. Dhabbe, A. N. Kadam, and K. M. Garadkar, "Enhanced photocatalytic activity of Ag doped TiO2 nanoparticles synthesized by a microwave assisted method," Ceram. Int., vol. 40, no. 4, pp. 5489–5496, 2014, doi: https://doi.org/10.1016/j.ceramint.2013.10.137

[19]   L. Elsellami, F. Dappozze, A. Houas, and C. Guillard, "Effect of Ag+ reduction on the photocatalytic activity of Ag-doped TiO2," Superlattices Microstruct., vol. 109, pp. 511–518, 2017, doi: https://doi.org/10.1016/j.spmi.2017.05.043

[20]   R. Solano, A. Herrera, D. Maestre, and A. Cremades, "Fe-TiO2 Nanoparticles Synthesized by Green Chemistry for Potential Application in Waste Water Photocatalytic Treatment," J. Nanotechnol., vol. 2019, pp. 1–11, 2019, doi: https://doi.org/10.1155/2019/4571848

[21]   M. A. Behnajady, N. Modirshahla, M. Shokri, and B. Rad, "Enhancement of photocatalytic activity of TiO2 nanoparticles by Silver doping: Photodeposition versus liquid impregnation methods," Glob. Nest J., vol. 10, no. 1, pp. 1–7, 2008, doi: https://doi.org/10.30955/gnj.000485

[22]   M. Pazoki, M. Parsa, and R. Farhadpour, "Removal of the hormones dexamethasone (DXM) by Ag doped on TiO2 photocatalysis," J. Environ. Chem. Eng., vol. 4, no. 4, pp. 4426–4434, 2016, doi: https://doi.org/10.1016/j.jece.2016.09.034

[23]   M. Malakootian, M. Pourshaban-Mazandarani, H. Hossaini, and M. H. Ehrampoush, "Preparation and characterization of TiO2 incorporated 13X molecular sieves for photocatalytic removal of acetaminophen from aqueous solutions," Process Saf. Environ. Prot., vol. 104, pp. 334–345, 2016, doi: https://doi.org/10.1016/j.psep.2016.09.018

[24]   J. J. Alvear-daza, J. Sanabria, J. A. Rengifo, and H. M. Gutierrez-zapata, "Simultaneous abatement of organics (2,4-dichlorophenoxyacetic acid) and inactivation of resistant wild and laboratory bacteria strains by photo-induced processes in natural groundwater samples," Sol. Energy, vol. 171, pp. 761–768, 2018, doi: https://doi.org/10.1016/j.solener.2018.07.026

[25]   R. Arumugam et al., "Scalable novel PVDF based nanocomposite foam for direct blood contact and cardiac patch applications," J. Mech. Behav. Biomed. Mater., vol. 88, no. June, pp. 270–280, 2018, doi: https://doi.org/10.1016/j.jmbbm.2018.08.020

[26]   T. M. S. Dawoud, V. Pavitra, P. Ahmad, A. Syed, and G. Nagaraju, "Photocatalytic degradation of an organic dye using Ag doped ZrO2 nanoparticles: Milk powder facilitated eco-friendly synthesis," J. King Saud Univ. - Sci., vol. 32, no. 3, pp. 1872–1878, 2020, doi: https://doi.org/10.1016/j.jksus.2020.01.040

[27]   D. Dey et al., "Systematic study on the effect of Ag doping in shaping the magnetic property of sol-gel derived TiO2 nanoparticles," Ceram. Int., no. March, 2020, doi: https://doi.org/10.1016/j.ceramint.2020.07.282

[28]   S.-L. Chiam, Q.-Y. Soo, S.-Y. Pung, and M. Ahmadipour, "Polycrystalline TiO2 particles synthesized via one-step rapid heating method as electrons transfer intermediate for Rhodamine B removal," Mater. Chem. Phys., vol. 257, no. January 2020, p. 123784, 2020, doi: https://doi.org/10.1016/j.matchemphys.2020.123784

[29]   R. Solano, D. Patiño-Ruiz, and A. Herrera, "Preparation of modified paints with nano-structured additives and its potential applications," Nanomater. Nanotechnol., vol. 10, pp. 1–17, 2020, doi: https://doi.org/10.1177/1847980420909188

[30] M. Algarín, M. Amaya, R. Solano, D. Patiño-Ruiz, and A. Herrera, "Synthesis of a magnetic iron oxide/zinc oxide engineered nanocatalyst for enhanced visible-light photodegradation of Cartasol brilliant violet 5BFN in aqueous solution," Nano-Structures and Nano-Objects, vol. 26, p. 100730, 2021, doi: https://doi.org/10.1016/j.nanoso.2021.100730

[31] N. F. A. Neto, K. N. Matsui, C. A. Paskocimas, M. R. D. Bomio, and F. V Motta, "Study of the photocatalysis and increase of antimicrobial properties of Fe3+ and Pb2+ co-doped ZnO nanoparticles obtained by microwave-assisted hydrothermal method," Mater. Sci. Semicond. Process., vol. 93, pp. 123–133, 2019, doi: https://doi.org/10.1016/j.mssp.2018.12.034

[32] R. Solano and A. Herrera, "Cypermethrin elimination using Fe-TiO2 nanoparticles supported on coconut palm spathe in a solar flat plate photoreactor," Adv. Compos. Lett., vol. 28, pp. 1–13, 2020, doi: https://doi.org/10.1177/2633366X20906164

[33] M. Lien, C. Hieu, C. Fu, and R. Juang, "Hybridizing Ag-Doped ZnO nanoparticles with graphite as potential photocatalysts for enhanced removal of metronidazole antibiotic from water," J. Environ. Manage., vol. 252, p. 109611, 2019, doi: https://doi.org/10.1016/j.jenvman.2019.109611

[34] V. R. Chelli, S. Chakraborty, and A. K. Golder, "Ag-doping on TiO2 using plant-based glycosidic compounds for high photonic efficiency degradative oxidation under visible light," J. Mol. Liq., vol. 271, pp. 380–388, 2018, doi: https://doi.org/10.1016/j.molliq.2018.08.140

[35] T. Ali, A. Ahmed, U. Alam, I. Uddin, P. Tripathi, and M. Muneer, "Enhanced photocatalytic and antibacterial activities of Ag-doped TiO2 nanoparticles under visible light," Mater. Chem. Phys., vol. 212, pp. 325–335, 2018, doi: https://doi.org/10.1016/j.matchemphys.2018.03.052

[36] S. P. Onkani, P. N. Diagboya, F. M. Mtunzi, M. J. Klink, B. I. Olu-owolabi, and V. Pakade, "Comparative study of the photocatalytic degradation of 2 – chlorophenol under UV irradiation using pristine and Ag-doped species of TiO2, ZnO and ZnS photocatalysts," J. Environ. Manage., vol. 260, p. 110145, 2020, doi: https://doi.org/10.1016/j.jenvman.2020.110145

[37] L. Mahmoudian-boroujerd, A. Karimi-jashni, and S. Nezamedin, "Optimization of rDNA degradation in recombinant Hepatitis B vaccine production plant wastewater using visible light excited Ag-doped TiO2 nanophotocatalyst," Process Saf. Environ. Prot., vol. 122, pp. 328–338, 2019, doi: https://doi.org/10.1016/j.psep.2018.11.027

[38] L. Elleuch et al., "A new insight into highly contaminated landfill leachate treatment using Kefir grains pre-treatment combined with Ag-doped TiO2 photocatalytic process," J. Hazard. Mater., vol. 382, p. 121119, 2020, doi: https://doi.org/10.1016/j.jhazmat.2019.121119

[39] M. Mel, M. Marques, and S. Paula, "Silver oxidation state effect on the photocatalytic properties of Ag doped TiO2 for hydrogen production under visible light," Int. J. Hydrogen Energy, vol. 40, pp. 17308–17315, 2015, doi: https://doi.org/10.1016/j.ijhydene.2015.09.058

[40] R. A. Solano Pizarro and A. P. Herrera Barros, "Cypermethrin elimination using Fe-TiO2 nanoparticles supported on coconut palm spathe in a solar flat plate photoreactor," Adv. Compos. Lett., vol. 28, pp. 1–13, 2020, doi: https://doi.org/10.1177/2633366X20906164

[41] C. J. Lin, W. T. Yang, C. Y. Chou, and S. Y. H. Liou, "Hollow mesoporous TiO2 microspheres for enhanced photocatalytic degradation of acetaminophen in water," Chemosphere, vol. 152, pp. 490–495, 2016, doi: https://doi.org/10.1016/j.chemosphere.2016.03.017

[42] G. Wang, L. Xu, J. Zhang, T. Yin, and D. Han, "Enhanced photocatalytic activity of TiO2 powders (P25) via calcination treatment," vol. 2012, pp. 1–9, 2012, doi: https://doi.org/10.1155/2012/265760

[43] A. G. El-Shamy, "An efficient removal of methylene blue dye by adsorption onto carbon dot @ zinc peroxide embedded poly vinyl alcohol (PVA/CZnO2) nano-composite: A novel Reusable adsorbent," Polymer (Guildf)., vol. 202, p. 122565, 2020, doi: https://doi.org/10.1016/j.polymer.2020.122565

[44] F. Pellegrino et al., "Influence of agglomeration and aggregation on the photocatalytic activity of TiO2 nanoparticles," Appl. Catal. B Environ., vol. 216, pp. 80–87, 2017, doi: https://doi.org/10.1016/j.apcatb.2017.05.046

[45] T. Zhang et al., "Enhanced photocatalytic activity of TiO2 with acetylene black and persulfate for degradation of tetracycline hydrochloride under visible light," Chem. Eng. J., vol. 384, p. 123350, 2020, doi: https://doi.org/10.1016/j.cej.2019.123350

[46] R. Solano, G. Cerri, A. Herrera, and X. Vargas, "Cr+6 and Zn+2 Removal for Heterogeneous Photocatalysis with TiO2 in Synthetic Wastewater," Int. J. ChemTech Res., vol. 11, no. 03, pp. 312–320, 2018, doi: https://doi.org/10.20902/IJCTR.2018.110342

[47] T. A. Kurniawan, L. Yanyan, T. Ouyang, A. B. Albadarin, and G. Walker, "BaTiO3/TiO2 composite-assisted photocatalytic degradation for removal of acetaminophen from synthetic wastewater under UV–vis irradiation," Mater. Sci. Semicond. Process., vol. 73, pp. 42–50, 2018, doi: https://doi.org/10.1016/j.mssp.2017.06.048

[48] L. Yanyan, T. A. Kurniawan, Z. Ying, A. B. Albadarin, and G. Walker, "Enhanced photocatalytic degradation of acetaminophen from wastewater using WO3/TiO2/SiO2 composite under UV–VIS irradiation," J. Mol. Liq., vol. 243, pp. 761–770, 2017, doi: https://doi.org/10.1016/j.molliq.2017.08.092

Green Synthesis of Silver-Doped Titanium Dioxide Nanostructures for Acetaminophen Degradation Under Solar Radiation

INGENIERÍA Y UNIVERSIDAD: ENGINEERING FOR DEVELOPMENT | COLOMBIA | V. 26 | 2022 | ISSN: 0123-2126/2011-2769 (Online) | Pag. 19